Electronic Supplementary Material (ESI) for Dalton Transactions.

Supplementary Information

For

Heteroaryl Bismuthines: A Novel Synthetic Concept and Metal···π Heteroarene Interaction

A. M. Preda,[a] W. B. Schneider,[a] M. Rainer,[a] T. Rüffer,[b] D. Schaarschmidt,[b]

H. Lang[b] and M. Mehring[a]*

[a)] Technische Universität Chemnitz, Fakultät für Naturwissenschaften, Institut für Chemie, Professur Koordinationschemie, 09107 Chemnitz, Germany

[b)] Technische Universität Chemnitz, Fakultät für Naturwissenschaften, Institut für Chemie, Professur Anorganische Chemie, Chemnitz, Germany

Table of content:

*Synthesis of [Bi{OCMe$_2$(2-C$_4$H$_3$S)}$_3$]$_2$ (**1**) and [Bi$_4$O$_2$(OCMe$_2$(2-C$_4$H$_3$S)}$_8$] (**2**)* ····3

Synthesis of Bi(OSiMe$_2$Ph)$_3$ ····3

*Solid state structure of [Bi{OCMe$_2$(2-C$_4$H$_3$S)}$_3$]$_2$ (**1**) and [Bi$_4$O$_2$(OCMe$_2$(2-C$_4$H$_3$S)}$_8$] (**2**)* ····4

Figure S3 *Molecular structure of Bi(2-C$_4$H$_2$S-5-SiMe$_3$)$_3$ (**5**)* ····6

Figure S4 *^{1}H NMR spectra in CDCl$_3$ at ambient temperature showing the formation of Bi(2-C$_4$H$_3$S)$_3$ (**4**)* ····7

Figure S5 *NMR spectra of Bi(OSiMe$_2$Ph)$_3$ in CDCl$_3$* ····8

Figure S6 *^{1}H NMR spectra of **1** and **2** in CDCl$_3$* ····9

Figure S7 *^{1}H NMR spectrum of Bi(2-C$_4$H$_3$O)$_3$ (**3**) in CDCl$_3$* ····9

Figure S8 *^{1}H NMR spectrum of Bi(2-C$_4$H$_3$S)$_3$ (**4**) in CDCl$_3$* ····10

Figure S9 *^{1}H NMR spectrum of Bi(2-C$_4$H$_2$S-5-SiMe$_3$)$_3$ (**5**) in CDCl$_3$* ····10

Figure S10 *^{1}H NMR spectrum of Bi(2-C$_4$H$_3$NMe)$_3$ (**6**) in CDCl$_3$* ····10

Figure S11 *^{1}H NMR spectrum of Bi(2-C$_4$H$_3$Se)$_3$ (**7**) in CDCl$_3$* ····11

Figure S12 *^{1}H NMR spectrum of Bi(3-C$_4$H$_3$S)$_3$ (**8**) in CDCl$_3$* ····11

Figure S13 *Powder X-ray diffraction pattern at 293 K of Bi(2-C$_4$H$_3$O)$_3$ (**3**)* ····12

Figure S14 *Powder X-ray diffraction pattern at 110 K of Bi(2-C$_4$H$_3$S)$_3$ (**4**)* ····12

Figure S15 *Powder X-ray diffraction pattern at 120 K of Bi(2-C$_4$H$_2$S-5-SiMe$_3$)$_3$ (**5**)* ····13

Figure S16 *Powder X-ray diffraction pattern at 110 K of Bi(2-C$_4$H$_3$NMe)$_3$ (**6**)* ····13

Figure S17 *Powder X-ray diffraction pattern at 120 K of Bi(2-C$_4$H$_3$Se)$_3$ (**7a**)* ····14

Figure S18 *Powder X-ray diffraction pattern at 293 K of Bi(2-C$_4$H$_3$Se)$_3$ (**7b**)* ····14

Figure S19 *Powder X-ray diffraction pattern at 293 K of Bi(3-C$_4$H$_3$S)$_3$ (**8**)* ····15

References ····15

Synthesis of $[Bi\{OCMe_2(2\text{-}C_4H_3S)\}_3]_2$ (1) and $[Bi_4O_2\{OCMe_2(2\text{-}C_4H_3S)\}_8]$ (2):

A solution of $HOCMe_2(2\text{-}C_4H_3S)$ (0.557 g, 3.91 mmol) in n-hexane (10 mL) was added dropwise to a solution of $Bi(O^tBu)_3$ (0.559 g, 1.30 mmol) in *n*-hexane (20 mL) at –20°C. After stirring overnight at ambient temperature a colourless precipitate was formed, which was filtered off and dried under vacuum. Yield: 0.354 g (54 %). Colourless single crystals for **1** were grown from a *n*-hexane solution that was partially reduced under vacuum (15 mL) and stored at –28 °C for a 1-2 days. **1**: M.p: 113–114 °C. Elemental analysis calcd. (%) for $C_{21}H_{27}BiO_3S_3$ (632.61 g·mol^{-1}): C, 39.9; H, 4.3; S, 15.2. Found: C, 39.1; H, 4.4; S, 14.5. Upon a longer time of crystallization and due to the presence of moisture partial hydrolysis of **1** in *n*-hexane solution at –28 °C afforded single crystals of **2** suitable for single crystals X-ray diffraction. **2:** M.p: 128–130 °C. Elemental analysis calcd. (%) for $C_{56}H_{72}Bi_4O_{10}S_8$ (1997.61 g·mol^{-1}): C, 33.7; H, 3.6; S, 12.8. Found: C, 33.4; H, 4.0; S, 12.5. ATR FTIR (cm^{-1}): *v* = 3071 (w), 2967 (m), 1465 (w), 1436 (w), 1364 (m), 1325 (w), 1240 (s), 1142 (vs) 1084 (w), 1054 (w), 1035 (w), 953 (s), 858 (m), 833 (m), 694 (vs), 631 (w), 527 (s, br), 494 (w), 419 (w). ^{1}H NMR (500 MHz, C_6D_6): δ 1.82 [s, 48H, H_7, $C(CH_3)_2$], 6.68 [dd, 8H, H_4, $^3J_{H\text{-}H}$ = 4.8 Hz, $^3J_{H\text{-}H}$ = 3.7 Hz, C_4H_3], 6.78 [d, 8H, H_3, $^3J_{H\text{-}H}$ = 4.6 Hz, C_4H_3], 6.88 [d, 8H, H_5, $^3J_{H\text{-}H}$ = 3.3 Hz, C_4H_3]. $^{13}C\{^1H\}$ NMR (125 MHz, C_6D_6): δ 36.05 [s, C_7, $C(CH_3)_2$], 74.49 [s, C_6, $C(CH_3)_2$], 122.98 (s, C_5), 124.05 (s, C_3), 127.17 (s, C_4), 159.49 (s, C_2). ^{1}H NMR (500 MHz, $CDCl_3$): δ 1.74 [s, 48H, H_7, $C(CH_3)_2$], 6.88 [dd, 8H, H_4, $^3J_{H\text{-}H}$ = 5.1 Hz, $^3J_{H\text{-}H}$ = 3.5 Hz, C_4H_3], 6.99 [d, 8H, H_3, $^3J_{H\text{-}H}$ = 3.5, $^4J_{H\text{-}H}$ = 1.2 Hz, C_4H_3], 7.12 [d, 8H, H_5, $^3J_{H\text{-}H}$ = 5.1, $^4J_{H\text{-}H}$ = 1.2 Hz, C_4H_3]. $^{13}C\{^1H\}$ NMR (125 MHz, $CDCl_3$): δ 35.48 [s, C_7, $C(CH_3)_2$], 73.47 [s, C_6, $C(CH_3)_2$], 123.13 (s, C_5), 124.39 (s, C_3), 127.20 (s, C_4), 158.53 (s, C_2). The resonances in the ^{1}H NMR spectrum of a solution of crystals of **1** dissolved in C_6D_6 or $CDCl_3$ do not differ from the resonances observed in the ^{1}H NMR spectrum of **2** (Figure S6).

Synthesis of $Bi(OSiMe_2Ph)_3$: A solution of $HOSiMe_2Ph$ (0.560 g, 3.67 mmol) in *n*-hexane (20 mL) was added dropwise to a solution of $Bi(O^tBu)_3$ (0.525 g, 1.22 mmol) in *n*-hexane (20 mL). After stirring for 3.5 h at ambient temperature all volatiles solvents were evaporated under vacuum to give a colourless oil. Yield: 0.759 g (94%). ^{1}H NMR (500 MHz, $CDCl_3$): δ 0.34 [s, 18H, $Si(CH_3)_2$], 7.36 [m, 9H, $H_{meta\,+\,para}$, C_6H_5], 7.55 [dd, 6H, H_{ortho}, $^3J_{H\text{-}H}$ = 7.6 Hz, $^4J_{H\text{-}H}$ = 1.9, Hz, C_6H_5]. $^{13}C\{^1H\}$ NMR (125 MHz, $CDCl_3$): δ 1.01 [s, $Si(CH_3)_2$], 127.86 (s, C_{meta}), 129.40 (s, C_{para}), 133.16 (s, C_{ortho}), 140.00 (s, C_{ipso}). $^{29}Si\{^1H\}$ NMR (99 MHz, $CDCl_3$): δ –1.26 (s). Elemental analyses could not be measured due to the high moisture sensitivity of the bismuth silanolate $Bi(OSiMe_2Ph)_3$.

*Solid state structure of [Bi{OCMe$_2$(2-C$_4$H$_3$S)}$_3$]$_2$ (**1**) and [Bi$_4$O$_2$(OCMe$_2$(2-C$_4$H$_3$S)}$_8$] (**2**)*

Single crystals of compound **1** suitable for single crystal X–ray diffraction analysis were grown from a *n*-hexane solution at –28 °C. Crystallographic data for **1** are given in Table 1, its molecular structure is shown in Figure S1, and selected bond lengths and bond angles are listed in the figure caption. The distance between the bismuth atom and the heteroarene$_{centroid}$ of 3.525 Å (green dashed line in Figure S1) is longer than the distance found in the related dimer of [Bi(OSiPh$_2$^{t}Bu)$_3$]$_2$, (Bi–arene$_{centroid}$ of 3.340 Å),[1] but shorter than the distance observed in the organometallic dimer [Bi(CH$_2$-2-Cl-C$_6$H$_4$)$_3$]$_2$ (Bi–arene$_{centroid}$ distance of 3.659 Å).[2] Nevertheless, with regard to other compounds showing bismuth···π arene interaction compound **1** shows a rather weak interaction.

In **1** the arrangement at the Bi atom is best described as distorted trigonal bipyramidal with [3+2] binding when taking into account the London dispersion type bismuth···π heteroarene interaction of 3.525 Å and the secondary Bi···O intermolecular coordination. Noteworthy, the sulfur atom is not coordinating but is taking part in the dispersion type interaction of the heteroaryl ligand.

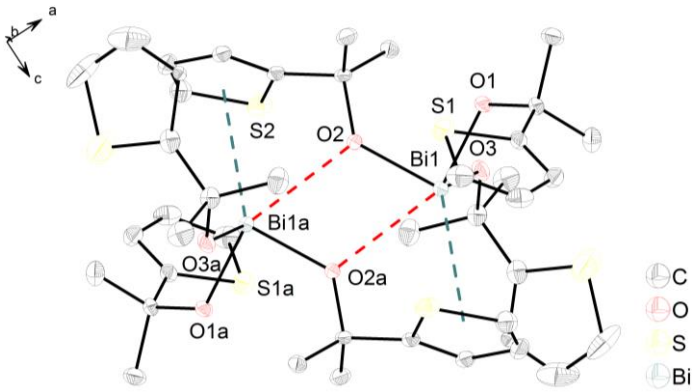

Figure S1 Molecular structure of the dimer [Bi{OCMe$_2$(2-C$_4$H$_3$S)}$_3$]$_2$ (**1**). Thermal ellipsoids are set at 30% probability level. Hydrogen atoms were omitted for clarity. For the disordered atoms, only one atomic position is shown. Symmetry transformations used to generate equivalent atoms: a = 1 – *x*, –*y*, –*z*. Selected bond lengths [Å]: Bi1–O1 2.105(2), Bi1–O2 2.097(2), Bi1–O3 2.093(2), Bi1–O2a 2.885(1), Bi1–heteroarene$_{centroid}$ 3.525. Selected bond angles [°]: O1–Bi1–O2 91.54(9), O1–Bi1–O3 87.7(1), O1–Bi1–O2a 144.3(1), O1–Bi1–heteroarene$_{centroid}$ 121.8, O2–Bi1–O3 96.1(1), O2–Bi1–O2a 67.4(1), O2–Bi1–heteroarene$_{centroid}$ 128.5, O3–Bi1–O2a 121.6(1), O3–Bi1–heteroarene$_{centroid}$ 120.9, Bi1–O2–Bi1a 112.6(1).

The tetranuclear compound **2** crystallizes from *n*-hexane solution at –28 °C in the triclinic space group $P\bar{1}$. Crystallographic data are given in Table 1, its molecular structure is shown in Figure 2 and selected bond lengths and angles are listed in the figure caption. The crystal structure of **2** is best described as being composed of a $[Bi_4O_2]^{8+}$ unit, where eight anionic [-OCMe$_2$-2-(C$_4$H$_3$S)]$^-$ ligands are coordinated

to bismuth (Figure S2). Bismuth oxido species,[3] especially those with ladder-type $[Bi_4O_6]$ moieties, *e.g.* $[Bi_4(\mu_3\text{-}O)_2(\mu\text{-}OSiEt_3)_6(OSiEt_3)_2]$,[4] $\{(ArO)_2Bi(\mu_3\text{-}O)Bi(\mu_2\text{-}O)\text{-}4\text{-}Br\text{-}2\text{-}^{i}Pr\text{-}6\text{-}[(C{=}CH_2)CH_2]C_6H_2\text{-}1{:}2\kappa^2O,2\kappa C\}_2$,[5] $[Bi_2(\mu_3\text{-}O)(OCH(CF_3)_2)_2(\mu\text{-}OCH(CF_3)_2)_2(C_7H_8)]_2$,[6] $[Bi_4O_2(HC_8)]$ (HC_8 = calix[8]arene),[7] $[Bi_4O_2(BnC_8)]$ (BnC_8 = *para*-benzylcalix[8]arene),[7] $[Bi_8O_4(^{t}BuC_8)_2]$ (^{t}BuC8 = *p-tert*-butylcalix[8]arene)[8] and $[Bi_4(\mu_3\text{-}O)_2(HO\text{-}2\text{-}C_6H_4CO_2)_8]\cdot 2MeCN$[9] were reported.

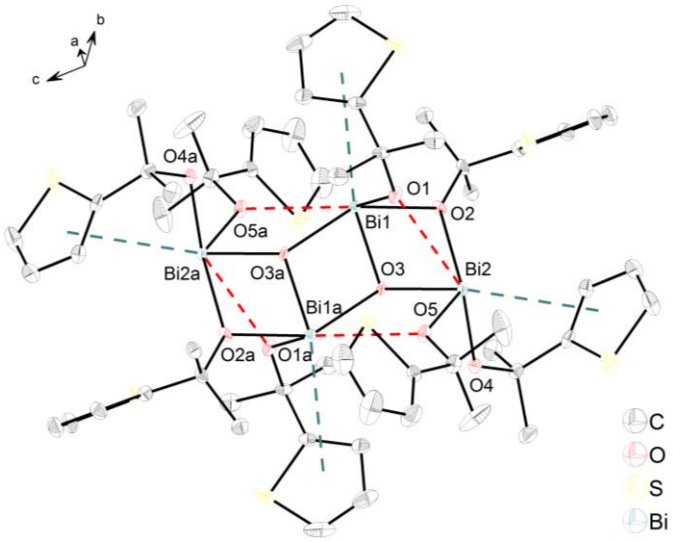

Figure S2 Molecular structure of $[Bi_4(\mu_3\text{-}O)_2(\mu\text{-}OCMe_2\text{-}2\text{-}C_4H_3S)_6(OCMe_2\text{-}2\text{-}C_4H_3S)_2]$ (**2**). Thermal ellipsoids are set at 30% probability level. Hydrogen atoms were omitted for clarity. Symmetry transformations used to generate equivalent atoms: a = $-x$, $-y$, $1-z$. Selected bond lengths [Å]: Bi1–O1 2.117(4), Bi1–O2 2.209(4), Bi1–O3 2.095(4), Bi1–O3a 2.426(4), Bi1–O5a 2.905, Bi2–O1 2.891, Bi2–O2 2.759(4), Bi2–O3 2.077(4), Bi2–O4 2.101(4), Bi2–O5 2.126(5), Bi1–Bi2 3.420(5), Bi1–Bi1a 3.655(5), Bi1–Bi2a 3.868, Bi1–heteroarene$_{centroid}$ 3.811, Bi2–heteroarene$_{centroid}$ 3.752. Selected bond angles [°]: O1–Bi1–O2 84.8(2), O1–Bi1–O3 81.2(2), O1–Bi1–O3a 85.0(2), O1–Bi1–O5a 137.3(1), O2–Bi1–O3 76.3(2), O2–Bi1–O3a 148.1(1), O2–Bi1–O5a 137.7, O3–Bi1–O3a 72.3(2), O2–Bi2–O3 64.9(2), O2–Bi2–O4 109.2(2), O2–Bi2–O5 141.0(1), O3–Bi2–O4 88.7(2), O3–Bi2–O5 81.3(2), O4–Bi2–O5 88.10(2), Bi1–Bi2–O1 81.6(1), Bi1–Bi2–O2 40.1(9), Bi1–Bi2–O3 35.1(1), Bi1–Bi2–O4 118.2 (1), Bi1–Bi2–O5 100.82(1), Bi1–Bi1a–O3 33.1(9), Bi2–Bi1–Bi1a 66.2(9), Bi2–Bi1–Bi2a 120.2(8), Bi1–Bi2–Bi1a 59.8(7), Bi1–Bi2–Bi2a 31.9(5).

Similar to compound **1** four thienyl moieties are found in close proximity to bismuth atoms and might be considered to stabilize the cluster by London dispersion type bismuth···π heteroarene interaction. If this weak force is taken into account, a highly distorted octahedral environment at the bismuth atoms, with Bi–heteroarene$_{centroid}$ bond distances (green dashed line in Figure S2) of 3.811 Å for Bi1 and 3.752 Å for Bi2, is observed. Similar to **1** the distances between the bismuth centres and the

centroids of the thienyl rings in **2** are well within the range reported for bismuth···π arene interactions (*i.e.* the distances between bismuth and the centroid of the ring are given in the range 2.96–3.93 Å).[10] However, the bismuth···π heteroarene interactions are in the upper range of typical distances for this type of interaction and thus bismuth–oxygen interactions dominate the interactions with the bismuth atoms.

The metal–metal distances for **2** amount to Bi1–Bi2 3.420(5) Å, Bi1–Bi1a 3.655(5) Å, Bi1–Bi2a 3.868 Å and Bi1a–Bi2a 3.420(5) Å, and are thus significantly shorter than the well-accepted sum of the van der Waals radii of two bismuth atoms [Σr_{vdW}(Bi,Bi) 4.80 Å].[11, 12] One possible explanation for this might be the presence of dispersion type Bi–Bi interactions within bismuth oxido unit.

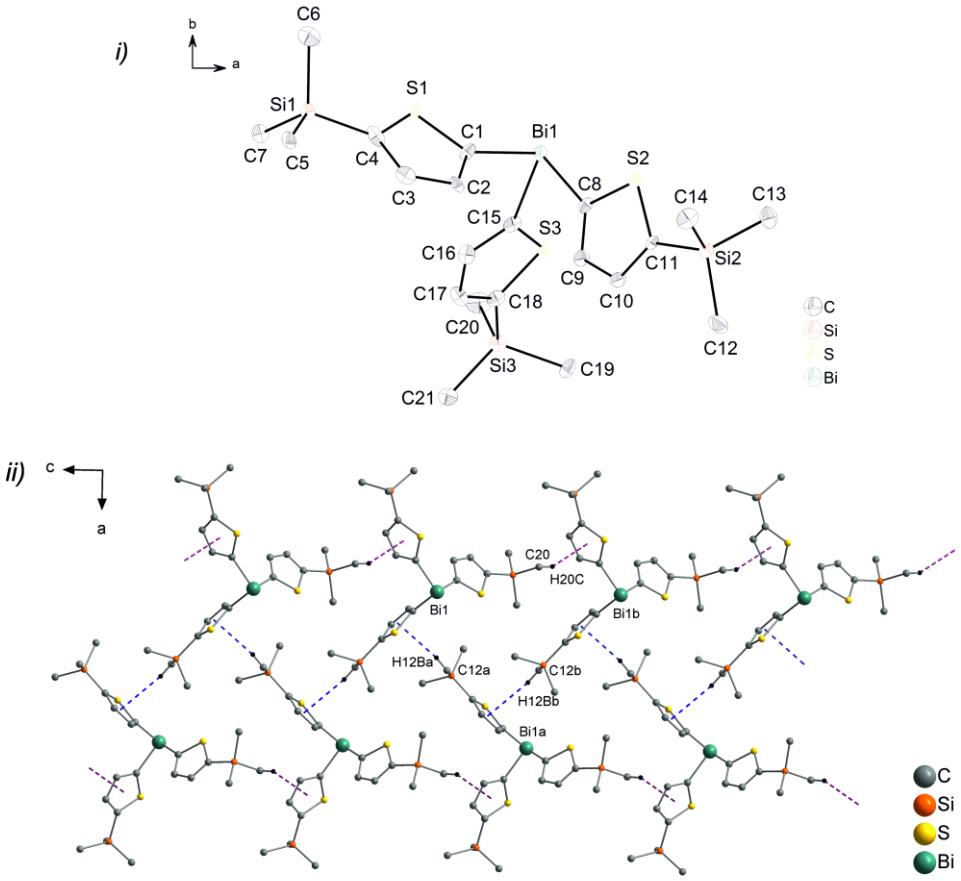

Figure S3 Molecular structure of Bi(2-C_4H_2S-5-$SiMe_3$)$_3$ (**5**). i) Thermal ellipsoids are set at 30% probability level. Hydrogen atoms were omitted for clarity. Selected bond lengths [Å]: Bi1–C1 2.211(16), Bi1–C8 2.217(14), Bi1–C15 2.206(15). Selected bond angles [°]: C1–Bi1–C8 93.7(5), C1–Bi1–C15 92.5(6), C8–Bi1–C15 90.6(5); ii) Ball and stick model of the molecular structure of **5**, showing the formation of a 2D network of two helical chains via C–H_{methyl}···π (heteroarene$_{centroid}$) intermolecular interactions with C12–H12Ba$_{methyl}$···π (heteroarene$_{centroid}$) 2.996 Å (blue dashed line) and zig-zag chain C20–H20C$_{methyl}$···π (heteroarene$_{centroid}$) 3.096 Å (purple dashed line) [only hydrogen atoms involved in C–H_{methyl}···π(heteroarene$_{centroid}$) interactions are shown]. Symmetry transformation: a = 1 – *x*, –*y*, –½ + *z*; b = *x*, *y*, –1 + *z*.

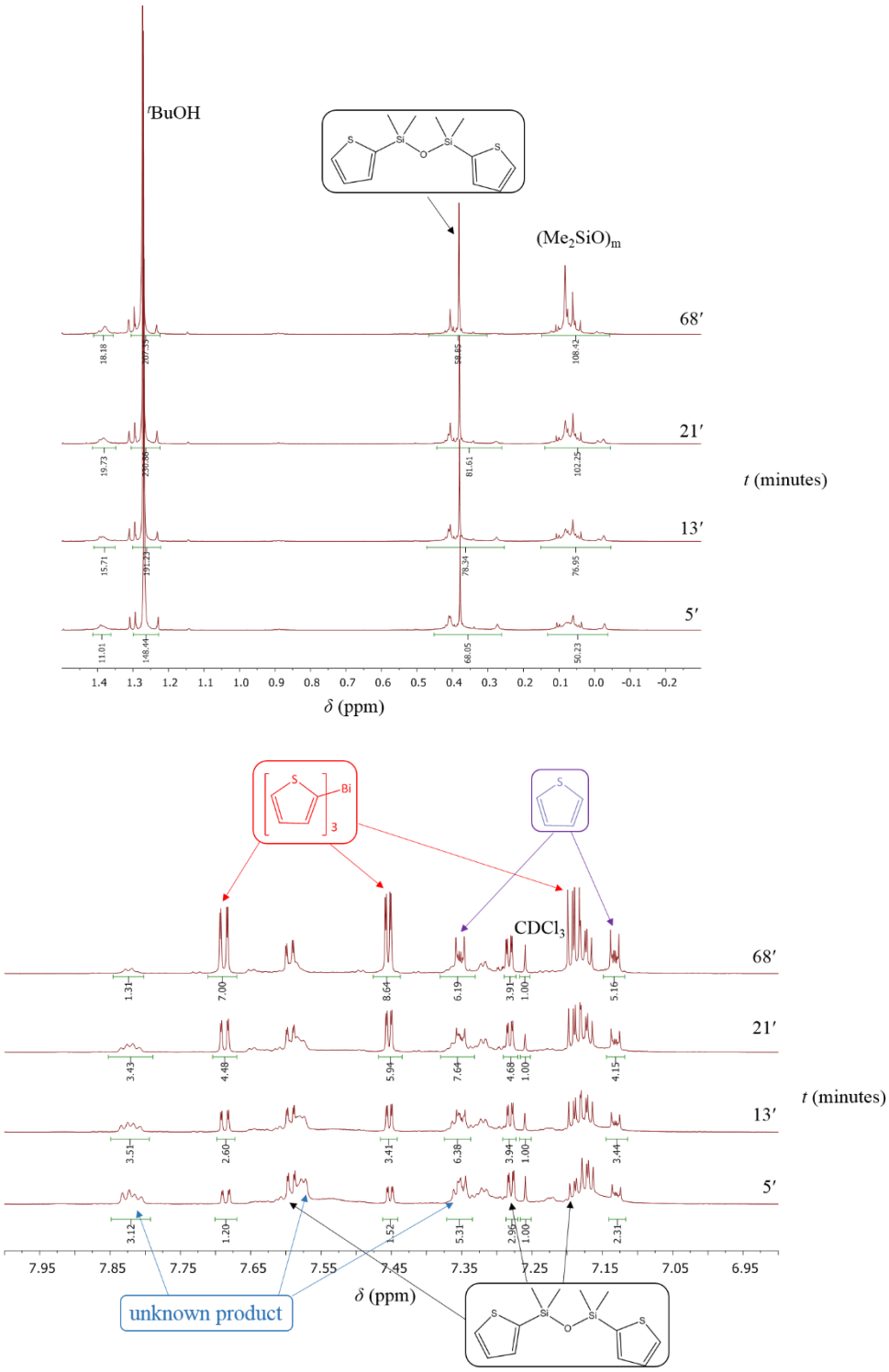

Figure S4 ^{1}H NMR spectra in $CDCl_3$ at ambient temperature of a mixture of $HOSiMe_2(2\text{-}C_4H_3S)$ and $Bi(O^tBu)_3$ (3:1) showing the formation of $Bi(2\text{-}C_4H_3S)_3$ (**4**) and the corresponding byproducts: aliphatic region (top); aromatic region (bottom).

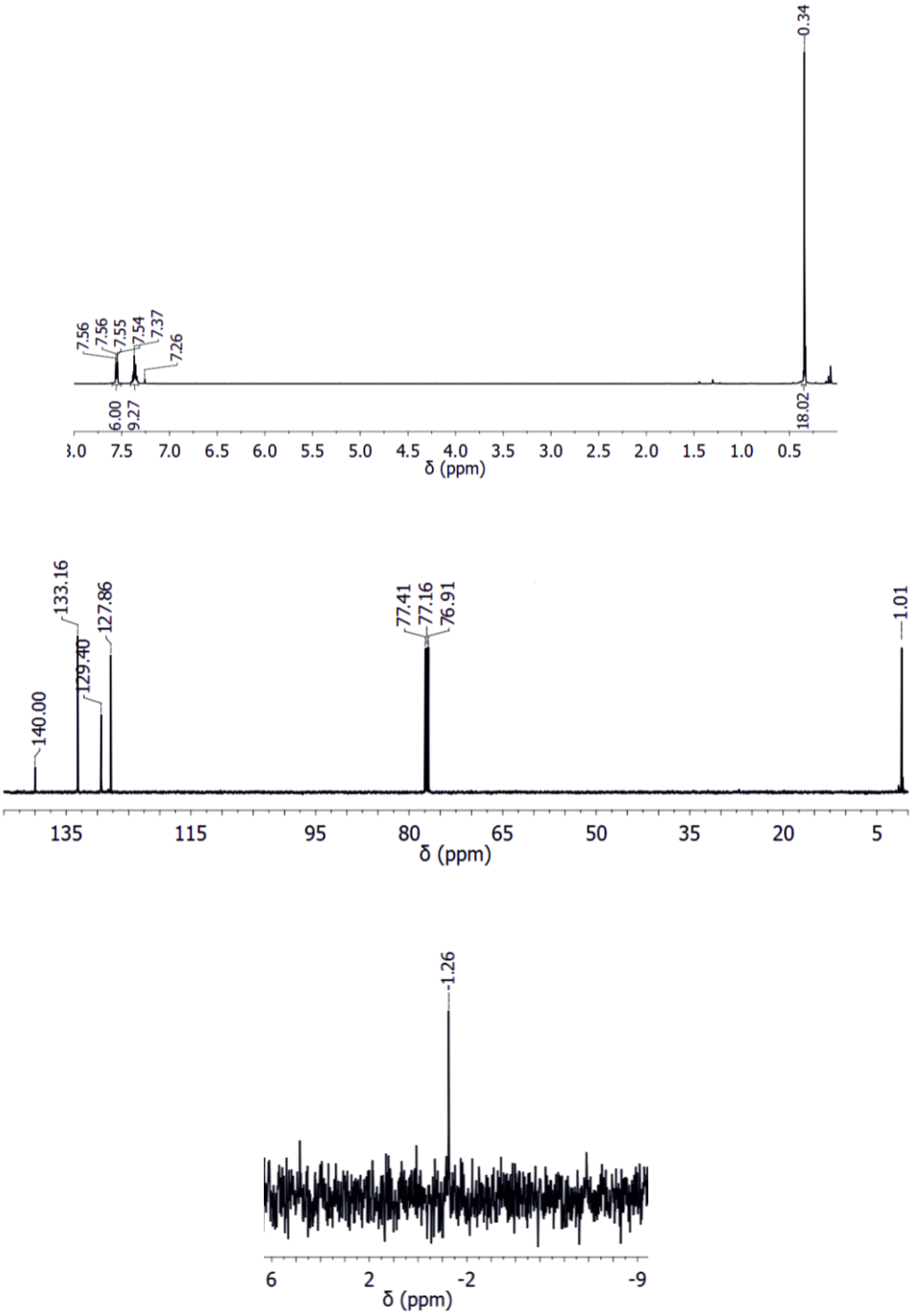

Figure S5 NMR spectra of $Bi(OSiMe_2Ph)_3$ in $CDCl_3$, at ambient temperature: ^{1}H NMR (top), b) $^{13}C\{^{1}H\}$ NMR (middle), $^{29}Si\{^{1}H\}$ NMR (bottom).

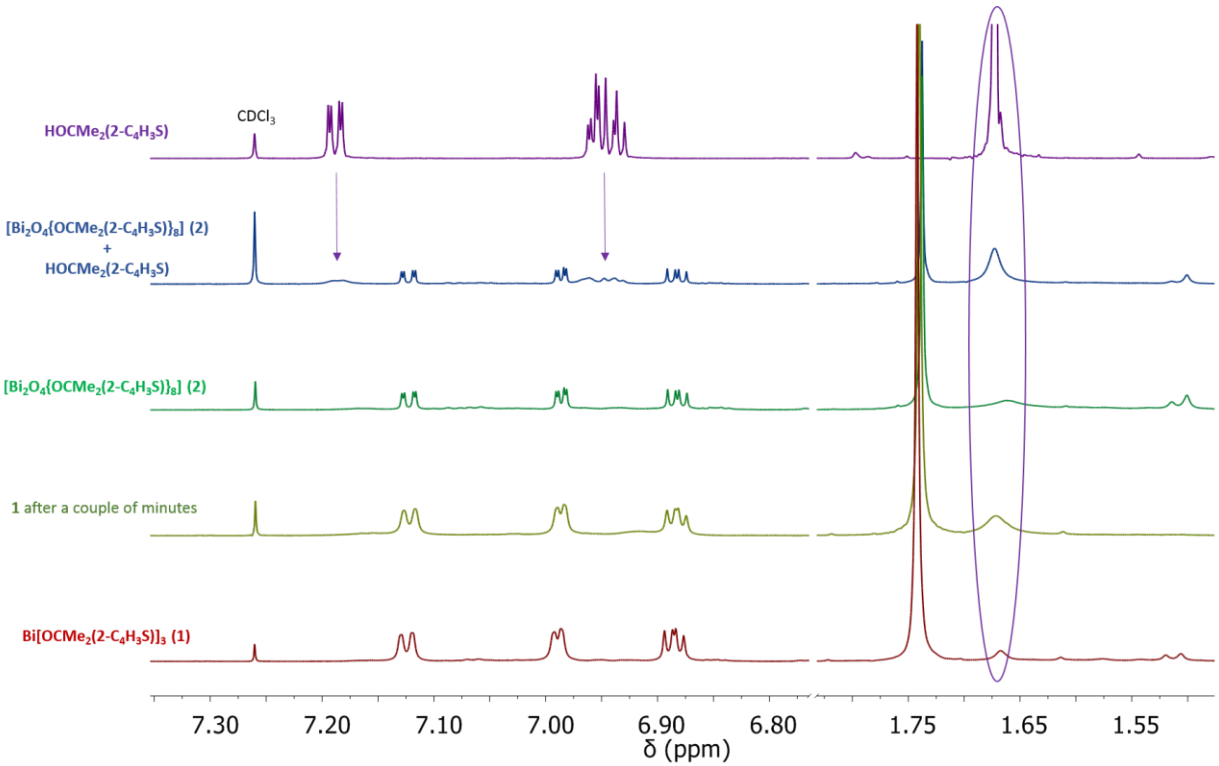

Figure S6 ^{1}H NMR spectra of **1** and **2** in $CDCl_3$, at ambient temperature exposed to air moisture.

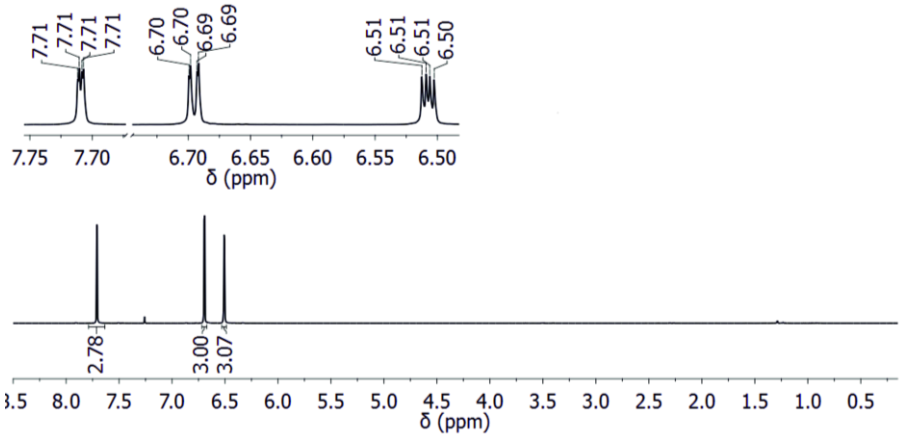

Figure S7 ^{1}H NMR spectrum of $Bi(2\text{-}C_4H_3O)_3$ (**3**) in $CDCl_3$, at ambient temperature.

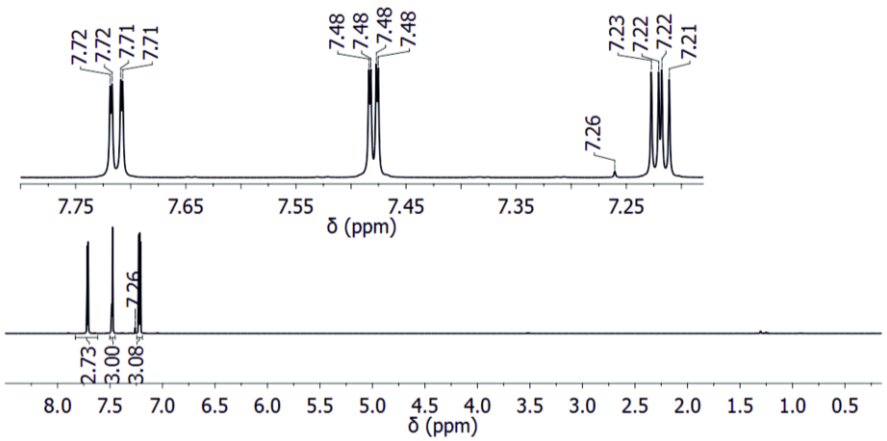

Figure S8 ^{1}H NMR spectrum of Bi(2-C_4H_3S)$_3$ (**4**) in $CDCl_3$, at ambient temperature.

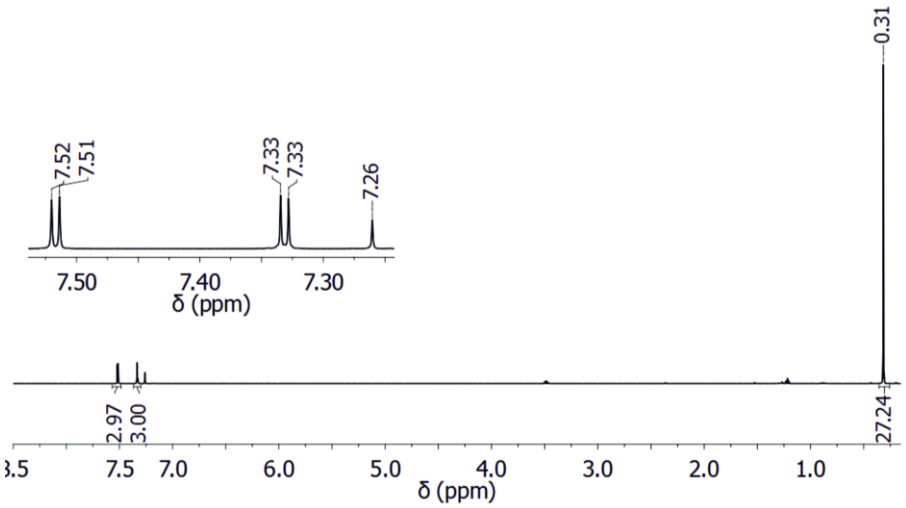

Figure S9 ^{1}H NMR spectrum of Bi(2-C_4H_2S-5-$SiMe_3$)$_3$ (**5**) in $CDCl_3$, at ambient temperature.

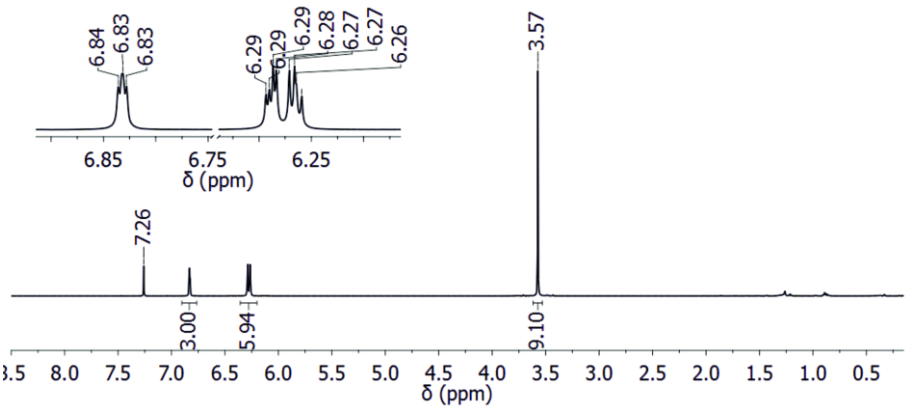

Figure S10 ^{1}H NMR spectrum of Bi(2-C_4H_3NMe)$_3$ (**6**) in $CDCl_3$, at ambient temperature.

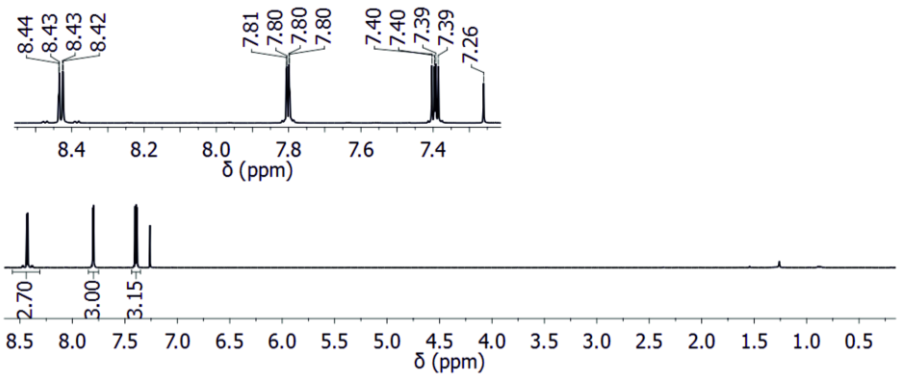

Figure S11 ^{1}H NMR spectrum of Bi(2-$C_4H_3Se)_3$ (**7**) in $CDCl_3$, at ambient temperature.

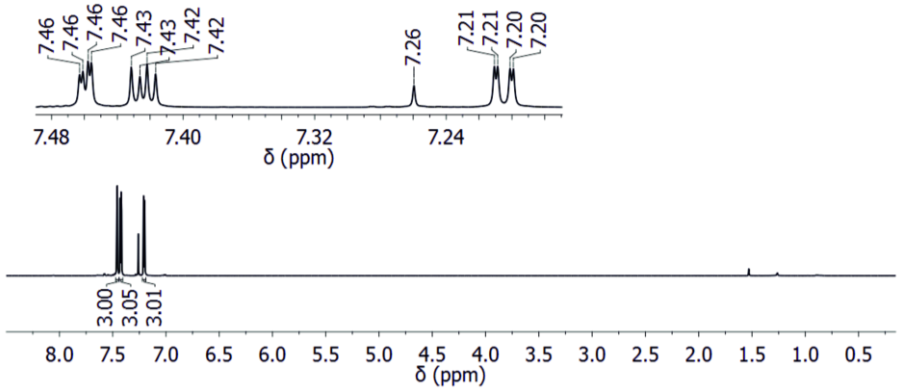

Figure S12 ^{1}H NMR spectrum of Bi(3-$C_4H_3S)_3$ (**8**) in $CDCl_3$, at ambient temperature.

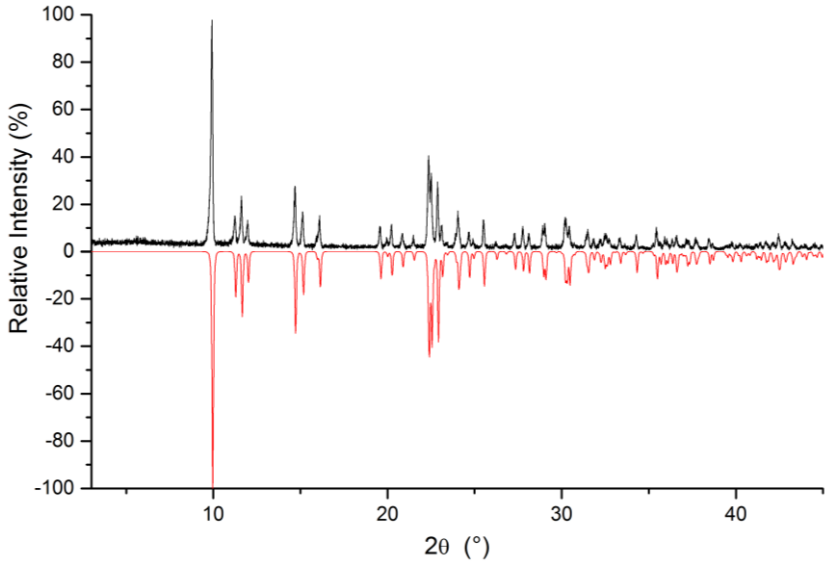

Figure S13 Powder X-ray diffraction pattern at 293 K of $Bi(2\text{-}C_4H_3O)_3$ (**3**), measured (black line) and calculated from single crystal X-ray data measured at 293 K (red line).[13]

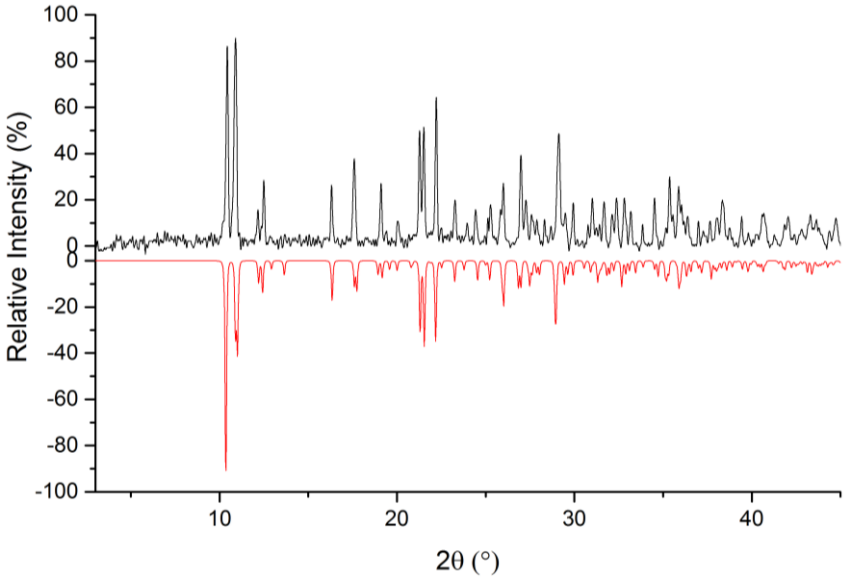

Figure S14 Powder X-ray diffraction pattern at 110 K of $Bi(2\text{-}C_4H_3S)_3$ (**4**), measured (black line) and calculated from single crystal X-ray data measured at 100 K (red line).

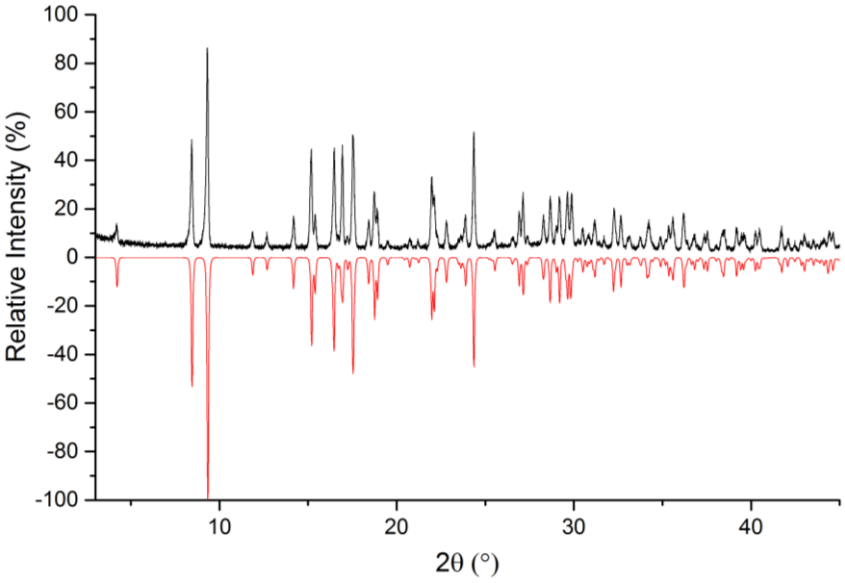

Figure S15 Powder X-ray diffraction pattern at 120 K of Bi(2-C_4H_2S-5-$SiMe_3$)$_3$ (**5**), measured (black line) and calculated from single crystal X-ray data measured at 120 K (red line).

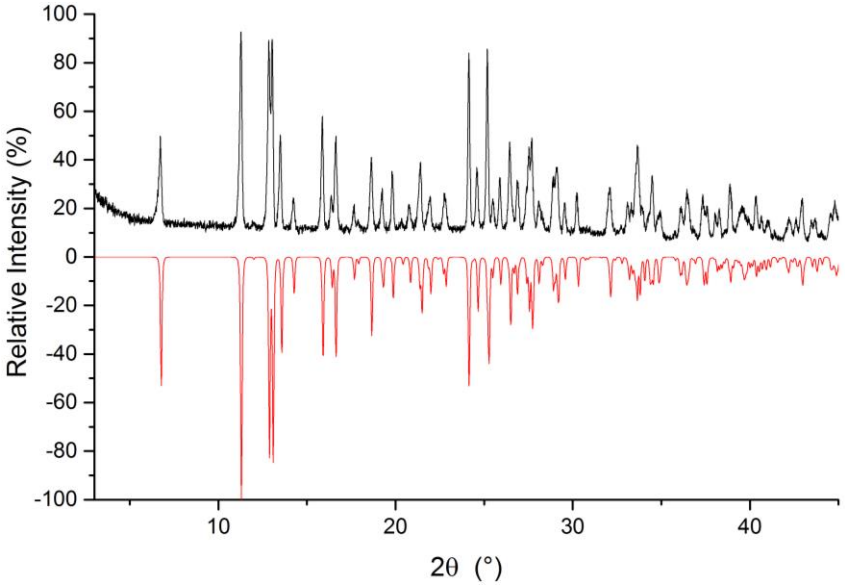

Figure S16 Powder X-ray diffraction pattern at 110 K of Bi(2-C_4H_3NMe)$_3$ (**6**), measured (black line) and calculated from single crystal X-ray data measured at 110 K (red line).

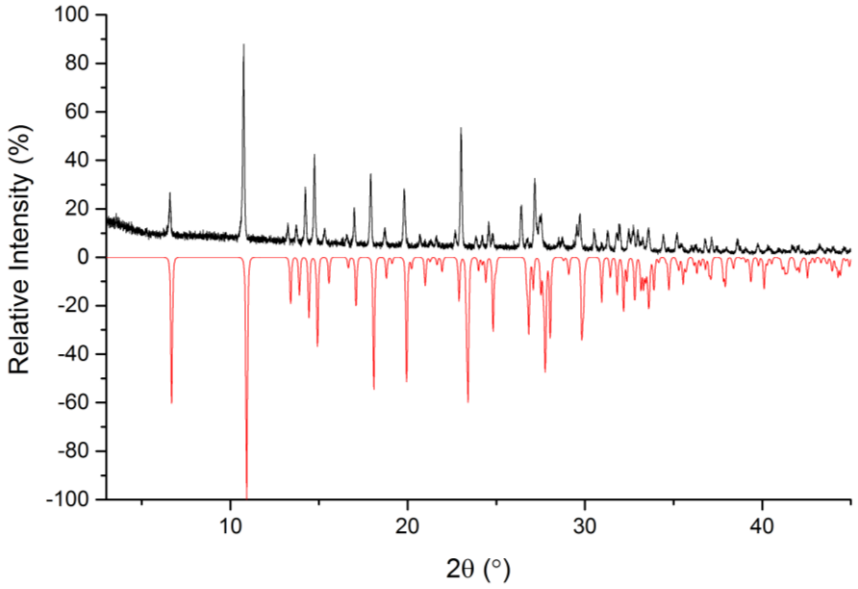

Figure S17 Powder X-ray diffraction pattern at 120 K of Bi(2-$C_4H_3Se)_3$ (**7a**), measured (black line) and calculated from single crystal X-ray data measured at 120 K (red line).

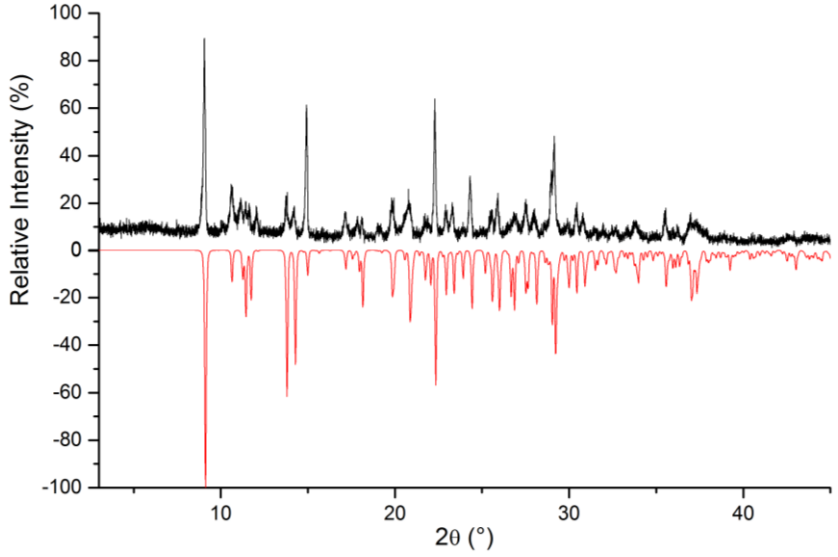

Figure S18 Powder X-ray diffraction pattern at 293 K of Bi(2-$C_4H_3Se)_3$ (**7b**), measured (black line) and calculated from single crystal X-ray data measured at 293 K (red line).[14]

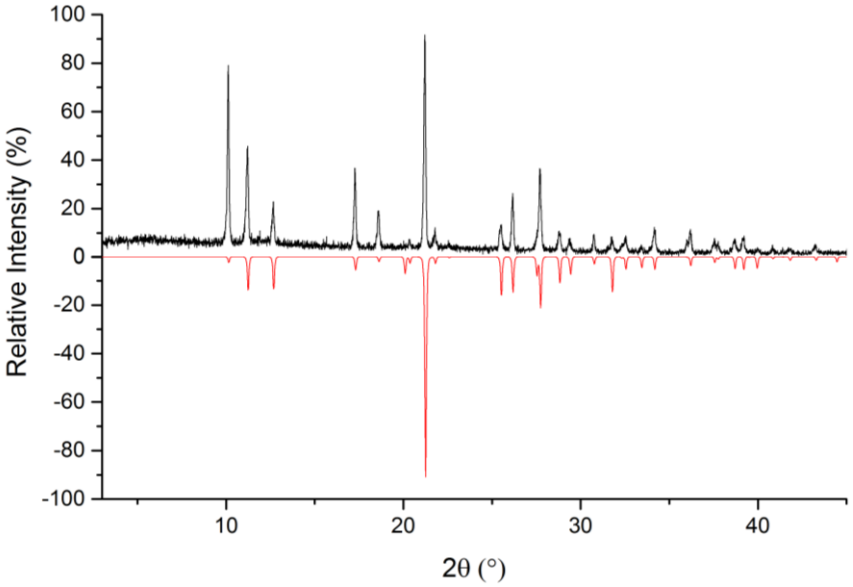

Figure S19 Powder X-ray diffraction pattern at 293 K of $Bi(3\text{-}C_4H_3S)_3$ (**8**), measured (black line) and calculated from single crystal X-ray data measured at 293 K (red line).[15] The intensity of the first reflection is different due to the preferred orientation of the plate like crystals.

References:

1. D. Mansfeld, M. Mehring and M. Schürmann, *Z. Anorg. Allg. Chem.*, 2004, **630**, 1795-1797.
2. A. A. Auer, D. Mansfeld, C. Nolde, W. Schneider, M. Schürmann and M. Mehring, *Organometallics*, 2009, **28**, 5405-5411.
3. M. Mehring, in *Clusters – Contemporary Insight in Structure and Bonding*, ed. S. Dehnen, Springer International Publishing, Cham, 2016, vol. 174, pp. 201-268.
4. M. Mehring, D. Mansfeld, S. Paalasmaa and M. Schürmann, *Chem. Eur. J.*, 2006, **12**, 1767-1781.
5. X. Kou, X. Wang, D. Mendoza-Espinosa, L. N. Zakharov, A. L. Rheingold, W. H. Watson, K. A. Brien, L. K. Jayarathna and T. A. Hanna, *Inorg. Chem.*, 2009, **48**, 11002-11016.
6. P. C. Andrews, P. C. Junk, I. Nuzhnaya and L. Spiccia, *Dalton Trans.*, 2008, 2557-2568.
7. D. Mendoza-Espinosa, A. L. Rheingold and T. A. Hanna, *Dalton Trans.*, 2009, 5226-5238.
8. L. Liu, L. N. Zakharov, A. L. Rheingold and T. A. Hanna, *Chem. Commun.*, 2004, 1472-1473.
9. T. D. Boyd, I. Kumar, E. E. Wagner and K. H. Whitmire, *Chem. Commun.*, 2014, **50**, 3556-3559.
10. H. Schmidbaur and A. Schier, *Organometallics*, 2008, **27**, 2361-2395.
11. N. C. Norman, in *Chemistry of Arsenic, Antimony and Bismuth*, Blackie, London, 1st edn., 1998.
12. A. Bondi, *J. Phys. Chem.*, 1964, **68**, 441-451.
13. P. S. Adela Lemus, Armando Cabrera, N. Rosas, Cecilio Alvarez, E. Gomez, Manju Sharma, C. Cespedes, S. Hernandez, *Main Group Met. Chem.*, 2001, **24**, 835-840.
14. P. Sharma, N. Rosas, A. Cabrera, A. Toscano, M. d. J. Silva, D. Perez, L. Velasco, J. Perez and R. Gutierez, *J. Organomet. Chem.*, 2005, **690**, 3286-3291.
15. P. Sharma, N. Rosas, A. Cabrera, M. J. S. Hernandez, A. Toscano, S. Hernández and R. Gutierrez, *Appl. Organomet. Chem.*, 2005, **19**, 1121-1126.